NIH Public Access
Author Manuscript
Cell Metab. Author manuscript; available in PMC 2010 June 25.

Published in final edited form as:
Cell Metab. 2009 October ; 10(4): 260–272. doi:10.1016/j.cmet.2009.08.009.

Reactive oxygen species enhance insulin sensitivity

Kim Loh[1], **Haiyang Deng**[1], **Atsushi Fukushima**[1], **Xiaochu Cai**[1], **Benoit Boivin**[2], **Sandra Galic**[1], **Clinton Bruce**[3], **Benjamin J. Shields**[1], **Beata Skiba**[3], **Lisa M. Ooms**[1], **Nigel Stepto**[4], **Ben Wu**[1], **Christina A. Mitchell**[1], **Nicholas K. Tonks**[2], **Matthew J. Watt**[4], **Mark A. Febbraio**[3], **Peter J. Crack**[5], **Sofianos Andrikopoulos**[6], and **Tony Tiganis**[1,7]

[1] Department of Biochemistry and Molecular Biology, Monash University, Victoria 3800, Australia

[2] Cold Spring Harbor Laboratory, Cold Spring Harbor, NY 11724, USA

[3] Baker IDI Heart and Diabetes Institute, Victoria 8008, Australia

[4] Department of Physiology, Monash University, Victoria 3800, Australia

[5] Department of Pharmacology, The University of Melbourne, Victoria 3010, Australia

[6] Department of Medicine Heidelberg Repatriation Hospital, The University of Melbourne, Victoria 3081, Australia

SUMMARY

Chronic reactive oxygen species (ROS) production by mitochondria may contribute to the development of insulin resistance, a primary feature of type 2 diabetes. In recent years it has become apparent that ROS generation in response to physiological stimuli such as insulin may also facilitate signaling by reversibly oxidizing and inhibiting protein tyrosine phosphatases (PTPs). Here we report that mice lacking one of the key enzymes involved in the elimination of physiological ROS, glutathione peroxidase 1 (Gpx1), were protected from high fat diet-induced insulin resistance. The increased insulin sensitivity in Gpx1−/− mice was attributed to insulin-induced phosphatidylinositol-3-kinase/Akt signaling and glucose uptake in muscle and could be reversed by the anti-oxidant N-acetylcysteine. Increased insulin signaling correlated with enhanced oxidation of the PTP family member PTEN, which terminates signals generated by phosphatidylinositol-3-kinase. These studies provide causal evidence for the enhancement of insulin signaling by ROS *in vivo*.

Oxidative stress, or the chronic generation of ROS, is thought to contribute to the progression of various human diseases including type 2 diabetes. Oxidative stress in such diseased states is primarily a bi-product of normal oxidative phosphorylation chemistry in mitochondria. Superoxide ($O2^{\bullet -}$), a natural bi-product of the single electron transport chain is generated at complex I and at complex III (Kim et al., 2008; Veal et al., 2007). $O2^{\bullet -}$ is converted to the ROS H_2O_2 by superoxide dismutase and then to oxygen and water by anti-oxidant enzymes such catalase, thioredoxin and glutathione peroxidases (Gpxs). In type 2 diabetes and conditions of morbid obesity, the increased supply of energy substrates and the inflammatory environment is thought to result in excessive mitochondrial ROS generation to activate protein kinase signaling pathways that suppress the insulin signal downstream of the insulin receptor (IR) at the level of IR substrate-1 (IRS-1) and phosphatidylinositol-3-kinase (PI3K) to promote ‘insulin resistance’ (Kim et al., 2008; Newsholme et al., 2007; Veal et al., 2007).

[7]Corresponding author: Tony Tiganis, Department of Biochemistry and Molecular Biology, P.O. BOX 13D, Monash University, Vic. 3800, Australia., Tel: 61 3 9902 9332, Fax: 61 3 9902 9500, Tony.Tiganis@med.monash.edu.au.
S.G. current address: St Vincent’s Institute, Victoria 3065, Australia.
B.W. current address: Heart Research Institute, NSW 2050, Australia
N.S. current address: Victoria University, Victoria 3011, Australia

NIH-PA Author Manuscript
NIH-PA Author Manuscript
NIH-PA Author Manuscript

NIH-PA Author Manuscript

NIH-PA Author Manuscript

NIH-PA Author Manuscript

Although the excessive production of ROS is associated with the pathology of many human diseases, in recent years it has become apparent that low levels of H_2O_2 may in fact be required for normal cellular functioning and intracellular signaling. Such physiological ROS is generated primarily at the plasma membrane and endomembranes by NADP(H) oxidases (Veal et al., 2007). A wide variety of stimuli including growth factors and hormones can promote the transient generation of H_2O_2 and this has been shown to be essential for optimal tyrosine phosphorylation-dependent signaling *in vitro* (Rhee, 2006; Tonks, 2006). Principal targets of ROS for promoting tyrosine phosphorylation-dependent signaling are the protein tyrosine phosphatases (PTPs) (Rhee, 2006; Tonks, 2006). The PTP superfamily includes phosphatases such as the prototypic PTP1B that dephosphorylate tyrosyl phosphorylated substrates and enzymes such as PTEN, which dephosphorylates phosphatidylinositol-3,4,5-triphosphate (PIP3) to terminate PI3K signaling. The architecture of the active site and the low thiol pKa of the invariant catalytic Cys renders PTPs highly susceptible to reversible oxidation by H_2O_2 (Tonks, 2006). The oxidation of the active site Cys abrogates its nucleophilic properties, thus rendering PTPs inactive. PTPs such as PTP1B and PTEN that regulate insulin sensitivity and glucose homeostasis *in vivo* (Elchebly et al., 1999; Wijesekara et al., 2005), are transiently oxidized by H_2O_2 in response to insulin in cell culture systems *in vitro* to promote IR activation and PI3K signaling respectively (Kwon et al., 2004; Lee et al., 2002; Mahadev et al., 2004; Meng et al., 2004; Seo et al., 2005). Whether ROS can contribute to the maintenance of insulin sensitivity *in vivo* via the inhibition of PTPs is unknown.

Gpx1 is a ubiquitous cytosolic and mitochondrial antioxidant enzyme that converts intracellular H_2O_2 to water using reduced glutathione as an electron donor (de Haan et al., 1998). In this study, we have taken advantage of mice that lack Gpx1 to examine the role of ROS in PTP regulation and insulin sensitivity and to establish the potential for ROS to act in a physiological context to suppress, rather than promote insulin resistance.

RESULTS

Enhanced ROS, PTEN oxidation and PI3K/Akt signaling in Gpx1−/− cells

We used mouse embryo fibroblasts (MEFs) isolated from Gpx1−/− versus +/+ mice (Fig. 1) and determined whether insulin-induced ROS levels and consequent signaling were altered. We found that insulin (10–100 nM)-induced H_2O_2 was elevated in Gpx1−/− MEFs but suppressed by the H_2O_2 scavenger and Gpx1 mimetic ebselen (Fig. 1a; data not shown). Although Gpx1 also has the capacity to detoxify lipid hydroperoxides (Ho et al., 1997), we saw no overt differences in lipid peroxidation in Gpx1−/− versus +/+ MEFs (data not shown). Insulin promotes IR β-subunit (IRβ) Y1162/Y1163 autophosphorylation and activation allowing for the phosphorylation of IRS-1 to recruit and activate the PI3K/Akt and Ras/mitogen-activated protein kinase (MAPK) pathways, which mediate the metabolic and mitogenic actions of insulin respectively. We found that the increased H_2O_2 levels in Gpx1−/− MEFs in response to insulin coincided with elevated PI3K/Akt signaling as measured by Akt Ser-473 phosphorylation (Fig. 1b) and this was suppressed by pre-treating cells with ebselen (Fig. 1c), the NADP(H) oxidase inhibitor diphenylene iodonium chloride (DPI) (Fig. 1c) or the anti-oxidant N-acetylcysteine (NAC; data not shown). Consistent with ROS serving in the fundamental control of insulin signaling, ebselen also suppressed insulin-induced ROS generation (Fig. 1a) and Akt Ser-473 phosphorylation in wild type MEFS (data not shown). We did not see any difference in the activation of the MAPK ERK1/2 in Gpx1−/− versus +/+ MEFs (Fig. 1b), indicating that signaling in general was not elevated. In addition, we did not see any global change in insulin-induced tyrosine phosphorylation in Gpx1−/− versus +/+ MEFs (data not shown) or differences in phosphorylation of IRβon Y1162/Y1163 (Fig. 1d). Consistent with this we did not see any significant difference in insulin-induced IRS-1 Y612 phosphorylation (Fig. 1e) or in the binding of the p85 subunit of PI3K to IRS-1 (data not

NIH-PA Author Manuscript

NIH-PA Author Manuscript

NIH-PA Author Manuscript

shown). Thus, the enhanced insulin-induced PI3K/Akt signaling cannot be ascribed to the insulin-induced oxidation of phosphotyrosine-specific PTPs such as PTP1B and TCPTP that dephosphorylate IRβ on Y1162/Y1163 (Galic et al., 2005) to terminate the insulin signal. Instead, these results point towards the elevated ROS acting downstream of IRβ and IRS-1 to selectively regulate PI3K/Akt signaling.

Previous studies have established that the PTP family member PTEN, which dephosphorylates the PI3K lipid product PIP3 to suppress downstream signaling and Akt activation can be oxidized and inhibited by H_2O_2 in response to insulin and platelet derived growth factor to promote PI3K/Akt signaling. The insulin-induced oxidation of PTEN results in enhanced PTEN electrophoretic mobility when resolved by SDS-PAGE (Kwon et al., 2004; Lee et al., 2002; Seo et al., 2005). Accordingly, we assessed the electrophoretic mobility of endogenous PTEN in Gpx1−/− versus +/+ MEFs in response to insulin or after the addition of exogenous H_2O_2 as a measure of PTEN oxidation. Exogenous H_2O_2 resulted in significant PTEN oxidation and concomitant Akt activation (Fig. 1f). In Gpx1+/+ MEFs, insulin induced the oxidation of PTEN to levels seen after the addition of 20–50 μM exogenous H_2O_2, an extracellular concentration of H_2O_2 thought to result in intracellular levels comparable to those achieved by physiological stimuli (Schroder and Eaton, 2008). Importantly, Gpx1-deficiency resulted in elevated and prolonged PTEN oxidation as monitored by the enhanced electrophoretic mobility in response to insulin (Fig. 1g). Furthermore, the enhanced PTEN oxidation in Gpx1−/− cells could be suppressed to basal levels by pre-treating cells with the NADP(H) oxidase inhibitor DPI (Fig. 1h), thus casually linking enhanced PTEN elecrophoretic mobility to the insulin-induced generation of ROS. Finally, we assessed PTEN oxidation directly using a modified cysteinyl-labelling technique that monitors the reversible oxidation of the active site Cys in PTPs (Boivin et al., 2008). Gpx1-deficiency resulted in the enhanced basal and insulin-induced oxidation of PTPs in general and consistent with our electrophoretic mobility experiments, in the enhanced oxidation of PTEN (Fig. 1i). Taken together, these results are consistent with Gpx1-deficiency resulting in elevated ROS levels to transiently oxidise and inhibit PTEN and thus promote PI3K/Akt signaling.

Enhanced insulin sensitivity in Gpx1−/− mice

Having established that Gpx1 deficiency can enhance insulin-induced PI3K/Akt signaling *in vitro* by inhibiting PTEN, we next examined the impact of Gpx1 deficiency on insulin sensitivity and glucose homeostasis *in vivo* (Fig. 2). Gpx1−/− mice are healthy and fertile and in the absence of oxidative challenge, such as that occurring under conditions of cerebral ischemia/reperfusion, do not show any overt histopathologies (Crack et al., 2001;de Haan et al., 1998;Ho et al., 1997). Male 8–10 week old Gpx1−/− versus +/+ mice were fed a standard chow diet for 12 weeks and insulin and glucose tolerances as well as fasted blood glucose and insulin levels determined. Although no overt differences were seen in insulin tolerance tests (ITTs) and glucose tolerance tests (GTTs), chow fed Gpx1−/− mice had modest, albeit significantly reduced fasted blood glucose levels and a tendency towards reduced insulin levels (Supplementary Fig. 1a, online), consistent with insulin sensitivity being enhanced. To examine this further we asked whether Gpx1 deficiency might enhance insulin sensitivity and afford protection from high fat diet-induced insulin resistance. Male and female 8–10 week old Gpx1−/− versus +/+ mice were fed a high fat diet (HFD) for a period of 12 weeks. Fasting plasma insulin levels increased (Fig. 2a) and the clearance of glucose in response to insulin was diminished in high fat fed +/+ mice consistent with the development of insulin resistance (data not shown). Insulin sensitivity, as measured in ITTs, was significantly enhanced in Gpx1 −/− mice independent of gender after high fat feeding (Fig. 2a–b). Glucose tolerance was improved in female mice (Supplementary Fig. 2a, online) and insulin levels during the GTTs were reduced in male mice (Supplementary Fig. 2b, online; data not shown) consistent with improved glucose handling. The improved insulin and glucose tolerances coincided with

NIH-PA Author Manuscript

NIH-PA Author Manuscript

NIH-PA Author Manuscript

significant reductions in fasted blood glucose and reduced fasted plasma insulin (Fig. 2a–b). Importantly, fasted plasma insulin in Gpx1-deficient mice was maintained at levels seen prior to high fat feeding (data not shown) or after 12 weeks of standard chow feeding (Fig. 2a). No significant difference was seen in plasma insulin levels from fed Gpx1−/− versus +/+ mice (Supplementary Fig. 2c, online) and no difference was evident in the initial increase in plasma insulin after bolus glucose administration (Supplementary Fig. 2b, online) indicating that pancreatic β cell insulin secretion was not altered as a result of Gpx1-deficiency. Instead, these results suggest that insulin sensitivity may be enhanced in Gpx1-deficient mice and that the mice are protected from high fat diet-induced insulin resistance. To explore this further, insulin sensitivity and glucose turnover were measured in high fat fed weight-matched Gpx1−/− versus +/+ male mice (Fig. 2c) by performing hyperinsulinaemic euglycaemic clamps (Fig. 2d–g). Insulin sensitivity, as measured by the glucose infusion rate during hyperinsulinemic-euglycemic clamps was increased by approximately three fold in Gpx1-deficient mice (Fig. 2d; Supplementary Fig. 3, online). In addition, insulin-stimulated glucose disappearance, which primarily reflects skeletal muscle glucose disposal, was increased in Gpx1−/− mice (Fig. 2d), whereas hepatic glucose production was not altered (Fig. 2e). Consistent with this, we found no overt difference between Gpx1−/− and +/+ mice in hepatic gluconeogenic gene expression as assessed by quantitative real-time PCR (Fig. 2f), whereas the uptake of 2-deoxy-[1-^{14}C]glucose was elevated by approximately 3–4 fold in Gpx1−/− white *gastrocnemius* and diaphragm skeletal muscles (Fig. 2g). Taken together, these results indicate that insulin sensitivity is elevated as a result of Gpx1-deficiency and that this may be attributed to the enhancement of insulin-induced glucose uptake in muscle.

PI3K/Akt signaling is enhanced in Gpx1−/− muscle

Our studies indicate that the enhanced insulin sensitivity in high fat fed Gpx1-deficient mice may be ascribed primarily to the increased responsiveness of muscle. To test this further, we assessed the activation of the IR and downstream signaling pathways in muscle, liver and fat. Gpx1−/− versus +/+ mice fed a HFD for 12 weeks were starved for 4 h and administered saline or insulin and tissues extracted for immunoblot analysis. We found that insulin-induced IRβ Y1162/Y1163 and IRS-1 Y612 phosphorylation were not altered in either muscle (Fig. 3a), liver, or fat from Gpx1−/− versus +/+ mice (data not shown). In contrast, an insulin-induced increase in PI3K/Akt signaling, as monitored by Akt Ser-473 phosphorylation (Fig. 3b; Supplementary Fig. 4a, online), was evident in muscle from Gpx1−/− but not +/+ mice, consistent with Gpx1 deficiency preventing the development of insulin resistance associated with high fat feeding. No difference was seen in the activation of the MAPKs ERK1/2, JNK and p38 in muscle (Supplementary Fig. 4b, online), consistent with the selective activation of the PI3K/Akt pathway. In line with the elevated PI3K/Akt signaling in Gpx1−/− muscle, we found that the phosphorylation of the Akt substrate of 160 kDa (AS160), a Rab GTPase that regulates GLUT4 docking at the plasma membrane for glucose uptake (Larance et al., 2005;Sano et al., 2003) was increased (Fig. 3c), whereas glycogen synthase Ser-640/641 phosphorylation was reduced (a consequence of Akt phosphorylating and inhibiting glycogen synthase kinase 3) (Fig. 3d). No significant difference in insulin-induced PI3K/Akt signaling was evident in liver or fat from Gpx1-deficient mice (Supplementary Fig. 4a, online). Consistent with this, we noted no significant difference in insulin signaling in hepatocytes isolated from Gpx1−/− versus +/+ mice (Supplementary Fig. 5a, online) or in −/− versus +/+ MEFs that had been differentiated into adipocytes *in vitro* (Supplementary Fig. 5b, online). In contrast, H_2O_2 levels as measured by DCF fluorescence ± ebselen and PI3K/Akt signaling in response to insulin (0.1–10 nM) were enhanced in Gpx1−/− versus +/+ myoblasts differentiated into multinucleated myotubes (Fig. 4a–b; data not shown); no overt difference was evident in the differentiation status of myotubes (data not shown). Consistent with the elevated PI3K/Akt signaling in Gpx1−/− myotubes, knockdown of Gpx1 (~50%) by RNA interference in C2C12 muscle cells also resulted in increased insulin-induced Akt Ser-473 phosphorylation and this

NIH-PA Author Manuscript

NIH-PA Author Manuscript

NIH-PA Author Manuscript

was suppressed by ebselen (Fig. 4c). In addition, consistent with our findings in muscle *in vivo*, insulin (1–100 nM) induced 2-deoxy-[1-^{14}C]glucose uptake was significantly elevated in Gpx1−/− myotubes (Fig. 4d; data not shown). Furthermore, as in MEFs, IRS-1 Y612 phosphorylation (Fig. 4b) and insulin-induced IRS-1 p85 PI3K recruitment (Fig. 4e) and PI3K activation (Fig. 4f) were not altered, but PTEN electrophoretic mobility was enhanced in Gpx1 −/− myotubes (Fig. 4g). Taken together, these results indicate that the enhanced insulin sensitivity in Gpx1−/− mice may be caused by increased ROS for the inactivation of PTEN and the enhancement of insulin-induced PI3K/Akt signaling and glucose uptake in muscle.

ROS promote insulin sensitivity in Gpx1−/− mice

Next, we asked whether the increased insulin-induced PI3K/Akt signaling in muscle and the enhanced insulin sensitivity in Gpx1−/− mice could be ascribed to increased ROS. We used Amplex Red to measure H_2O_2 levels in liver, muscle and fat extracts. We also measured H_2O_2 levels in blood plasma as an indicator of generalised oxidative stress. We found that H_2O_2 levels were elevated by approximately 3–4 fold in muscle, but not in liver or plasma (Fig. 5a); H_2O_2 could not be detected in fat using this approach (data not shown). We found no difference in SOD1 or catalase expression in muscle, liver or fat (Supplementary Fig. 6a, online) and no overt difference in muscle or liver catalase activity (Supplementary Fig. 6b, online). Consistent with the elevated H_2O_2, we found that the GSH/GSSG ratio (a reduced GSH/GSSG being an indicator of elevated ROS) was significantly reduced in Gpx1−/− muscle extracts (Fig. 5b), but lipid hydroperoxide levels remained unaltered in Gpx1−/− muscle, liver and fat (data not shown). Taken together, these results indicate that H_2O_2 levels may be elevated selectively in muscle as a result of Gpx1-deficiency.

Next we determined whether the elevated ROS was responsible for the enhanced PI3K/Akt signaling and insulin sensitivity. High fat fed male versus female Gpx1−/− versus +/+ mice were administered the anti-oxidant NAC (a H_2O_2 scavenger and stimulator of GSH production) for 7 days and either PI3K/Akt signaling assessed in muscle extracts after bolus insulin administration (Fig. 5d), or insulin sensitivity assessed in ITTs (Fig. 5e; Supplementary Fig. 7; online). NAC lowered muscle H_2O_2 and PI3K/Akt signaling in −/− mice to levels seen in +/+ mice (Fig. 5c–d). In addition, NAC administration increased fasted blood glucose in −/− mice and rendered −/− mice more insulin resistant so that they resembled +/+ mice, without having any overt effect on body weight (Fig. 5e; Supplementary Fig. 7; online); NAC did not alter insulin sensitivity in +/+ mice (Fig. 5e). These results provide causal evidence for the involvement of ROS in the enhancement of insulin signaling/sensitivity in high fat fed Gpx1 −/− mice *in vivo*.

Increased energy expenditure and obesity resistance in Gpx1−/− mice

In addition to increased insulin sensitivity, we found that Gpx1−/− mice were protected from high fat diet-induced obesity (Fig. 6). Gpx1-deficiency reduced epididymal and/or infrarenal fat accumulation in male and female high fat fed mice and this was associated with a decrease in body weight, but unaltered food intake (Fig. 6a–b). Epididymal adipocytes in Gpx1−/− mice were smaller in diameter (Fig. 6c) but their differentiation status as assessed by the expression of PPARγ, AP2 and C/EBP was similar to that of +/+ adipocytes (Supplementary Fig. 8a, online). In addition circulating adipokine levels were not affected (Supplementary Fig. 8b, online), the differentiation of MEFs into adipocytes *in vitro* remained unaltered (Fig. 6d) and insulin-induced lipogenesis in isolated fat pads *ex vivo* (Supplementary Fig. 8c, online) was not defective. Thus, these results are consistent with the decreased adiposity in Gpx1−/− mice being attributable to extrinsic factors. One possibility is that the decreased adiposity may be due to the enhanced insulin sensitivity and concomitant decreased plasma insulin, which otherwise promotes lipogenesis. In line with this Gpx1−/− remained more insulin sensitive than their wild type counterparts when the genotypes were weight-matched (Fig. 2;

NIH-PA Author Manuscript

NIH-PA Author Manuscript

NIH-PA Author Manuscript

Supplementary Fig. 9, online). Thus, these results are consistent with the increased insulin sensitivity in Gpx1−/− mice being independent of body weight and for the increased muscle insulin responsiveness being a possible driving factor for the lean phenotype.

Since food intake was identical but adiposity decreased in Gpx1−/− mice, we questioned how Gpx1−/− mice dealt with the apparent negative energy balance. First, we determined whether lipids were accumulated in liver and/or muscle and second assessed whether energy expenditure was altered in Gpx1-deficient mice. Plasma FFA and triglycerides and liver and muscle ceramides, diglycerides and triglycerides were not elevated in Gpx1−/− mice (Supplementary Fig. 10a–b, online; data not shown). Instead, high fat fed Gpx1−/− mice displayed increased energy expenditure (Fig. 6e) and whole body carbohydrate utilization (Fig. 6f). The enhanced energy expenditure could not be accounted for by changes in ambulatory movement (Fig. 6e) or any difference in brown adipose tissue mass (Fig. 6a–b) or the corresponding levels of UCP-1 (Supplementary Fig. 11a, online) that serves to uncouple the electron transport chain and dissipate energy as heat. Furthermore, the increase in energy expenditure was not associated with any change in muscle development (Supplementary Fig. 11b–c, online), muscle mass (data not shown), or muscle mitochondrial content and/or efficiency as assessed by measuring the activity of citrate synthase (citric acid cycle enzyme), UCP-3 levels (mitochondrial inner membrane protein), or directly by transmission electron microscopy (Supplementary Fig. 11d–f, online). No significant difference was observed in fat oxidation rates or in fatty acid oxidation *ex vivo* in liver, muscle or fat explants from fasted Gpx1−/− versus +/+ male or female mice (Supplementary Fig. 10c, online; data not shown).

Insulin-induced PI3K/Akt signaling decreases the expression of muscle pyruvate dehydrogenase kinase 4 (PDK4) that antagonizes pyruvate dehydrogenase, the rate limiting enzyme in glucose oxidation (Kim et al., 2006; Lee et al., 2004). Accordingly, we reasoned that the insulin-induced suppression of PDK4 may be enhanced and thus contribute to the increased carbohydrate utilization and energy expenditure in Gpx1−/− mice. Consistent with this, we found that *pdk4* mRNA (Fig. 6g) and protein (data not shown) levels were suppressed in diaphragm muscle from fasted Gpx1−/− but not +/+ mice after a single bolus administration of insulin (0.75 mU/g, 2 h). Although PDK4 expression in Gpx1−/− *gastrocnemius* muscle was not significantly altered under these conditions, a trend for reduced *pdk4* in response to insulin was evident (Fig. 6g). Taken together, these results indicate that Gpx1 deficiency affords resistance to diet-induced obesity and this is linked to increased energy expenditure which may result from the enhanced insulin-induced and PI3K/Akt-mediated suppression of PDK4 in muscle to promote carbohydrate utilization.

Sustained exercise-induced insulin sensitivity in Gpx1−/− mice

Our results indicate that a deficiency in Gpx1 mitigates the development of diet-induced insulin resistance by maintaining insulin sensitivity in muscle. Our studies using weight-matched mice and the anti-oxidant NAC indicate that the increased insulin sensitivity is separable from the concomitant obesity resistance. Nevertheless, we sought to establish an independent model by which to examine the impact of Gpx1 deficiency and elevated ROS on insulin sensitivity. Contracting muscle is a major source of physiological ROS *in vivo.* Although generated at mitochondria, exercise-induced ROS is transient and has been linked to the promotion of glucose uptake (Sandstrom et al., 2006). Furthermore, exercise can promote insulin sensitivity and this may occur downstream of the IR and IRS-1 at the level of the PI3K/Akt pathway (Wojtaszewski et al., 1999; Wojtaszewski et al., 2003; Zhou and Dohm, 1997). Therefore, we asked whether insulin sensitivity was enhanced in Gpx1−/− versus +/+ mice after a single bout of exercise. For these experiments we used chow fed mice where differences in body weight were not evident (Fig. 7). Chow fed Gpx1−/− and +/+ mice were starved for 12 h, exercised (30 min running at 16 m/min at a 5° incline) and then ITTs performed immediately after and

NIH-PA Author Manuscript

NIH-PA Author Manuscript

NIH-PA Author Manuscript

compared to those undertaken prior to exercise (Fig. 7a–b). Exercise increased insulin sensitivity, but there was no difference noted between the Gpx1−/− and +/+ mice (Fig. 7a–b). Since Gpx1 serves to eliminate low levels of ROS we reasoned that the impact of heightened ROS levels on insulin sensitivity in Gpx1−/− mice may be seen best after a period of rest, when ROS may be expected to decline in wild type mice. To test this hypothesis, exercised mice were rested for 1 h and ITTs performed. We found that insulin sensitivity in Gpx1−/− mice was significantly enhanced (Fig. 7c) and this coincided with elevated PI3K/Akt signaling as assessed by Akt Ser-473 phosphorylation (Fig. 7d). Next we asked whether the enhanced insulin sensitivity after rest could be attributed to sustained ROS. Gpx1−/− versus +/+ mice were administered the anti-oxidant NAC for 7 days and then exercised, rested and ITTs performed once more. We found that the enhanced insulin sensitivity in Gpx1−/− mice was reverted to that of +/+ mice but that insulin sensitivity in +/+ mice remained unaltered (Fig. 7e–f). These results are consistent with Gpx1-deficiency and sustained ROS levels prolonging/enhancing the beneficial effect of exercise on insulin responses.

DISCUSSION

Our studies demonstrate that increasing ROS, as a result of Gpx1-deficiency, can enhance insulin signaling *in vitro* and *in vivo* to attenuate the development of insulin resistance. Our results indicate that the enhanced ROS-dependent insulin signaling in Gxp1−/− MEFs and myotubes may be attributable to the oxidation and inhibition of the PTP superfamily member PTEN. Previous studies have shown that the catalytic active site Cys-124 in PTEN is readily oxidized by H_2O_2 to form a disulphide with Cys-71. Furthermore, PTEN oxidation can occur in cells in response to growth factors and insulin to promote Akt signaling (Kwon et al., 2004; Lee et al., 2002; Seo et al., 2005). Our studies suggest that PTEN is the primary, if not the sole ROS target that contributes to the enhanced insulin signaling in Gpx1−/− cells, since 1) PI3K/Akt signaling was increased downstream of PI3K, 2) PTEN was oxidised in response to insulin, and 3) PTEN is the only Cys-based lipid phosphatase that dephosphorylates the PIP3 product of PI3K to suppress insulin stimulated glucose uptake (Lazar and Saltiel, 2006; Wijesekara et al., 2005). The only other PIP3 phosphatases are the inositol polyphosphate 5-phosphatases that include SHIP1 and SHIP-2, but these do not belong to the PTP superfamily and do not contain a catalytic cysteine subject to oxidation (Hughes et al., 2000; Ooms et al., 2009). Although insulin-stimulated PTEN oxidation was modest, this is in keeping with 1) PTP regulation by ROS being discreet and compartmentalised (Chen et al., 2008; Ushio-Fukai, 2006), and 2) PTEN's role in diverse signalling pathways instigated by growth factors, hormones, cytokines and cell-cell/cell-matrix interactions. Furthermore, even though several tyrosine-specific PTPs have been implicated in the negative regulation of the IR and IRS-1 (Cho et al., 2006; Dubois et al., 2006; Elchebly et al., 1999; Galic et al., 2005), our results suggest that the oxidation of tyrosine-specific PTPs does not contribute to the enhanced insulin signaling in Gxp1−/− MEFs or mytotubes, since we saw no overt change in IR β-subunit Y1162/Y1163 and downstream IRS-1 phosphorylation and no difference in Ras/MAPK signaling, which occurs in parallel to the PI3K/Akt pathway. As in cells *in vitro* we found that the protection from diet-induced insulin resistance *in vivo* was associated with enhanced insulin sensitivity that was attributable to elevated ROS/PI3K/Akt signaling and consequent AS160 phosphorylation and glucose uptake in muscle, but unaltered IR and IRS-1 tyrosine phosphorylation and unaltered Ras/MAPK signaling. Although formally ascribing the enhanced insulin signaling to PTEN oxidation *in vivo* remains a challenge, our studies are in line with this possibility. Interestingly, we saw no difference in ITTs in chow fed Gpx1−/− mice. This is consistent with the phenotype of muscle-specific PTEN knockout mice, where increases in insulin sensitivity are only evident after aging or high fat feeding (Wijesekara et al., 2005). The apparent redundancy of PTEN in insulin responsiveness in the chow fed state would negate any impact of insulin-instigated PTEN oxidation and inhibition associated with Gpx1-deficiency.

NIH-PA Author Manuscript

NIH-PA Author Manuscript

NIH-PA Author Manuscript

Despite Gpx1 also being expressed in other tissues, widespread elevated H_2O_2 or oxidative stress was not apparent in Gpx1−/− mice and no difference was noted in PI3K/Akt signaling and consequent gluconeogenesis and lipogenesis in liver and fat respectively, pointing towards a functional redundancy. Although it is possible is that compensatory changes may have occurred in other anti-oxidant pathways, we saw no difference in SOD1 or catalase expression in liver or fat. Moreover, others have reported that other anti-oxidant enzymes are also not altered in Gpx1-deficient mice (de Haan et al., 2006; Ho et al., 1997). Interestingly, we found that hepatic catalase activity in wild type or knockout mice was several fold higher than that seen in muscle extracts. Therefore, one possibility is that the relative abundance/activities of other anti-oxidant enzymes in tissues such as the liver may readily counter any increase in H_2O_2 that would otherwise be associated with Gpx1 deficiency.

Previous studies have shown that Gpx1 overexpression in mice can result in insulin resistance and obesity (McClung et al., 2004). Although these results would appear to be consistent with our findings, subsequent studies from the same group have demonstrated that lean or obese Gpx1 overexpressing mice hyperproduce insulin and that isolated Gpx1 overexpressing islets hyper-secrete insulin in response to glucose (Wang et al., 2008). Since heightened insulin exposure has been linked with diminished insulin sensitivity (Rui et al., 2001; Weyer et al., 2000), it is likely that the peripheral insulin resistance and obesity reported for Gpx1 transgenic mice may be ascribed to the ROS induced overproduction of insulin in pancreatic β-cells. In our studies, Gpx1 deficiency did not overtly alter insulin production. In particular, we found that the initial increase in plasma insulin after bolus glucose administration was similar between the genotypes. Although insulin levels were lower in high fat fed mice after fasting, this can only be indicative of enhanced insulin sensitivity as reflected by the coincident reduction in blood glucose. We provided several lines of evidence to corroborate the enhanced insulin sensitivity. Although the hyperinsulinemic-euglycemic clamps were undertaken under anaesthesia, substantiating evidence was attained in ITTs and GTTs and in the assessment of insulin-induced signaling *in vivo* and *in vitro*. As such, our studies provide compelling evidence for ROS acting in peripheral insulin responsive tissues to enhance, rather than diminish insulin sensitivity *in vivo*.

In addition to enhanced insulin sensitivity we found that Gpx1−/− mice were protected from high fat diet-induced obesity. The obesity resistance was associated with increased whole body carbohydrate utilization, with no apparent decrease in fat oxidation. The increase in carbohydrate utilization correlated with the enhanced suppression of PDK4 in muscle. Previous studies have shown that insulin-induced PI3K/Akt signaling can suppress the expression of PDK4 to promote pyruvate dehydrogenase activity (Kim et al., 2006; Lee et al., 2004). Since Gpx1−/− mice were protected from high fat diet-induced insulin resistance and insulin-induced PI3K/Akt signaling and downstream PDK4 suppression were enhanced in muscle, we suggest that Gpx1−/− mice may remain lean, at least in part, due to the increased insulin-induced glucose uptake and carbohydrate oxidation in muscle; this would consequently decrease carbohydrate flux and lipogenesis in adipose tissue. Our studies indicate that the decreased adiposity in Gpx1−/− mice is not responsible for the enhanced insulin sensitivity since 1) the elevated insulin signaling was restricted to muscle, 2) the enhanced insulin sensitivity was evident in weight-matched mice, 3) NAC treatment diminished insulin sensitivity in Gpx1−/− mice to that of control mice without altering body weight, 4) the enhanced insulin responsiveness and glucose uptake in muscle could be recapitulated in myotubes *in vitro* and 5) Gpx1-deficiency prolonged the beneficial effects of exercise on insulin sensitivity in chow fed mice (where body weight did not differ) and this could be reversed by the anti-oxidant NAC. Therefore, these results support the assertion that Gpx1 deficiency and elevated ROS levels may promote insulin sensitivity independent of any change in body weight.

NIH-PA Author Manuscript

NIH-PA Author Manuscript

NIH-PA Author Manuscript

Although oxidative stress is generally linked with the development of disease, epidemiological studies in humans suggest that anti-oxidants may decrease life span (Bjelakovic et al., 2007), whereas other studies indicate that anti-oxidants may negate the longer term beneficial effects of exercise training in humans by preventing the expression of ROS defence genes (Ristow et al., 2009). This is consistent with our findings and the notion that ROS can serve as second messengers that are integral to fundamental cellular and biological responses (Rhee, 2006; Veal et al., 2007). However, this does not negate the involvement of chronic ROS in the progression of diseases such as diabetes. There are extensive markers associating ROS with obesity/diabetes in humans and many *in vitro* studies demonstrating that ROS can contribute to insulin resistance by activating protein kinase cascades that directly impinge on the propagation of signaling past IRS-1 (Newsholme et al., 2007). Furthermore, direct evidence for the involvement of hyperglycemia or obesity-induced ROS in promoting insulin resistance has been provided using mouse and rat animal models (Anderson et al., 2009; Haber et al., 2003; Houstis et al., 2006). In particular, the anti-oxidant MnTBAP improves insulin sensitivity in *ob/ob* mice that are excessively obese, hyperglycemic and insulin resistant (Houstis et al., 2006), whereas inhibiting muscle mitochondrial ROS generation in high fat fed rodents prevents hyperglycemia and insulin resistance (Anderson et al., 2009). So why then does Gpx1-deficiency and consequent elevated ROS enhance insulin sensitivity? We surmise that it is the degree of ROS generation and the context that determines whether ROS enhance or suppress insulin sensitivity. Whereas transient ROS produced by physiological stimuli such as insulin may be beneficial, sustained mitochondrial ROS generation associated with hyperglycemia and/or hyperlipidemia in obesity/diabetes may promote insulin resistance. Anderson *et al.* (2009) have reported that a high fat diet can increase glucose-induced mitochondrial ROS production in muscle. The high fat diet utilized in our studies promoted insulin resistance, but not hyperglycemia or severe obesity. Thus, we surmise the pathological levels of mitochondrial ROS associated with high fat feeding and increased energy substrate availability might not be achieved. We propose that our studies might reflect the contribution of ROS to insulin sensitivity early in the development of insulin resistance, prior to the onset of hyperglycemia/hyperlipidemia and frank diabetes. In summary, our studies provide casual evidence for the enhancement of insulin signaling by ROS *in vivo* and suggest that subtle increases in physiological ROS production in muscle might be of therapeutic benefit for the treatment of insulin resistance.

METHODS

Animal Maintenance and Experimental Protocols

We maintained mice on a 12 h light-dark cycle in a temperature-controlled facility with free access to food and water. Gpx1−/− (de Haan et al., 1998) and +/+ mice (C57BL/6) were fed standard chow (19% protein, 4.6% fat and 4.8% crude fibre) or high fat (19.5% protein, 36% fat and 4.7% crude fibre; Specialty Feeds) diets as indicated. See SI Methods for details for ITT, GTT and exercise experiments. Metabolic monitoring was performed in a Comprehensive Lab Animal Monitoring System (Columbus Instruments) as described in SI Methods. Hyperinsulinaemic-euglycaemic clamps were performed on anesthetized mice after overnight fasting and glucose uptake determined at the end of the clamp after bolus 2-[1-^{14}C]-deoxyglucose administration as described in SI Methods.

Cell culture

MEFs were isolated and cultured as described previously (Shields et al., 2008). Hepatocytes were isolated by a two step collagenase A (0.05% w/v) perfusion as described in SI Methods and cultured in M199 medium containing 10 % (v/v) heat inactivated FBS plus antibiotics (100 U/ml penicillin, 100 μg/ml streptomycin) and 1 nM insulin. Where indicated, cells were starved in medium alone for 6 h. Myoblasts were isolated from the muscle of 2–4 week old mice and

NIH-PA Author Manuscript

NIH-PA Author Manuscript

NIH-PA Author Manuscript

cultured in Ham's F10 medium containing 20% (v/v) heat inactivated FBS, antibiotics and 2.5 ng/ml human basic FGF as described in SI Methods. Cells were differentiated into multinucleated myotubes in DME medium containing 5% (v/v) horse serum (Sigma-Aldrich) plus antibiotics for 5 days. Where indicated, cells were starved in DME medium for 12 h. [^{3}H]2-deoxyglucose uptake in response to insulin (0–100 nM, 30 min) was determined as described previously (Watt et al., 2006). C2C12 immortalised myoblasts (ATCC) were cultured in DME medium containing 20% (v/v) FBS. For stable knockdown of Gpx1, control or Gpx1 specific shRNA lentiviral particles (Sigma-Aldrich) were used to transduce C2C12 cells according to the manufacturer's instructions and cells selected in 2 μg/ml puromycin.

ROS Determinations

Intracellular H_2O_2 was measured in serum starved MEFs or myotubes loaded with 10 μM CM-H_2DCF-DA and stimulated with 0.1–10 nM insulin as described in SI Methods. H_2O_2 levels in tissue extracts or plasma were determined using the Amplex Red hydrogen peroxide assay kit (Invitrogen) whereas GSH/GSSG ratios were determined using a BIOXYTECH GSH/GSSG-412 assay kit (Oxis International Inc).

Reversible PTP oxidation

PTP oxidation was monitored using a modified cysteinyl-labelling technique (Boivin et al., 2008). Oxidised α-bromobenzylphosphonate (BBP)-biotin-labelled PTPs were enriched on streptavidin-sepharose and precipitates resolved and immunoblotted using with streptavidin-horseradish peroxidase or PTEN-specific antibodies as described in SI Methods.

Biochemical analyses

Tissues were mechanically homogenized in 10–20 volumes of ice cold RIPA lysis buffer (50 mM Hepes pH 7.4, 1% (v/v) Triton X-100, 1% (v/v) sodium deoxycholate, 0.1% (v/v) SDS, 150 mM NaCl, 10% (v/v) glycerol, 1.5 mM MgCl_2, 1 mM EGTA, 50 mM NaF, leupeptin (5 μg/ml), pepstatin A (1 μg/ml), 1 mM benzamadine, 2 mM phenylmethysulfonyl fluoride, 1 mM sodium vanadate) and clarified by centrifugation (100, 000 × g, 20 min, 4°C). Cells were lysed in RIPA buffer plus/minus 50 mM NEM and clarified by centrifugation (16,000 × g, 5 min, 4°C). For IRS-1 immunoprecipitations, cells were lysed in NP-40 lysis buffer (50 mM Tris pH 7.4, 1% (v/v) NP-40, 200 mM NaCl, 50 mM NaF, leupeptin (5 μg/ml), pepstatin A (1 μg/ml), 1 mM benzamadine, 2 mM phenylmethysulfonyl fluoride, 1 mM sodium vanadate) and processed as described previously (Tiganis et al., 1998). PI3K assays were performed as described previously (Kong et al., 2000).

Real time PCR

Tissues were dissected and immediately frozen in liquid N_2 and RNA extracted using Trizol reagent (Invitrogen). mRNA was reversed transcribed using High Capacity cDNA Reverse Transcription Kit (Applied Biosystems) and quantitative real-time PCR using the TaqMan™ Universal PCR Master Mix and TaqMan™ Gene Expression Assays (Applied Biosystems). Relative quantification was achieved using the ΔΔCt method.

Statistical Analysis

A two-tailed Student's t test was used to test for differences between genotypes ortreatments. *$p < 0.05$, **$p < 0.01$, ***$p < 0.001$.

Supplementary Material

Refer to Web version on PubMed Central for supplementary material.

NIH-PA Author Manuscript

NIH-PA Author Manuscript

NIH-PA Author Manuscript

Acknowledgments

We thank Christine Yang, Moses Zhang, Teresa Tiganis, Debbie Lane, Amy Blair, Ray Spark, Robert Southgate and Ian Harper for technical support. This work was supported by the NH&MRC of Australia (to TT, MAF, PJC, SA, MJW, CAM), Diabetes Australia Research Trust (to TT) and the NIH (to NKT; CA53840, GM55989). CB, MJW, MAF and TT are NH&MRC research fellows.

References

Anderson EJ, Lustig ME, Boyle KE, Woodlief TL, Kane DA, Lin CT, Price JW 3rd, Kang L, Rabinovitch PS, Szeto HH, et al. Mitochondrial H2O2 emission and cellular redox state link excess fat intake to insulin resistance in both rodents and humans. J Clin Invest. 2009

Bjelakovic G, Nikolova D, Gluud LL, Simonetti RG, Gluud C. Mortality in randomized trials of antioxidant supplements for primary and secondary prevention: systematic review and meta-analysis. JAMA 2007;297:842–857. [PubMed: 17327526]

Boivin B, Zhang S, Arbiser JL, Zhang ZY, Tonks NK. A modified cysteinyl-labeling assay reveals reversible oxidation of protein tyrosine phosphatases in angiomyolipoma cells. Proc Natl Acad Sci U S A 2008;105:9959–9964. [PubMed: 18632564]

Chen K, Kirber MT, Xiao H, Yang Y, Keaney JF Jr. Regulation of ROS signal transduction by NADPH oxidase 4 localization. J Cell Biol 2008;181:1129–1139. [PubMed: 18573911]

Cho CY, Koo SH, Wang Y, Callaway S, Hedrick S, Mak PA, Orth AP, Peters EC, Saez E, Montminy M, et al. Identification of the tyrosine phosphatase PTP-MEG2 as an antagonist of hepatic insulin signaling. Cell Metab 2006;3:367–378. [PubMed: 16679294]

Crack PJ, Taylor JM, Flentjar NJ, de Haan J, Hertzog P, Iannello RC, Kola I. Increased infarct size and exacerbated apoptosis in the glutathione peroxidase-1 knockout mouse brain in response to ischemia/reperfusion injury. J Neurochem 2001;78:1389–1399. [PubMed: 11579147]

de Haan JB, Bladier C, Griffiths P, Kelner M, O'Shea RD, Cheung NS, Bronson RT, Silvestro MJ, Wild S, Zheng SS, et al. Mice with a homozygous null mutation for the most abundant glutathione peroxidase, Gpx1, show increased susceptibility to the oxidative stress-inducing agents paraquat and hydrogen peroxide. J Biol Chem 1998;273:22528–22536. [PubMed: 9712879]

de Haan JB, Witting PK, Stefanovic N, Pete J, Daskalakis M, Kola I, Stocker R, Smolich JJ. Lack of the antioxidant glutathione peroxidase-1 does not increase atherosclerosis in C57BL/J6 mice fed a high-fat diet. J Lipid Res 2006;47:1157–1167. [PubMed: 16508038]

Dubois MJ, Bergeron S, Kim HJ, Dombrowski L, Perreault M, Fournes B, Faure R, Olivier M, Beauchemin N, Shulman GI, et al. The SHP-1 protein tyrosine phosphatase negatively modulates glucose homeostasis. Nat Med 2006;12:549–556. [PubMed: 16617349]

Elchebly M, Payette P, Michaliszyn E, Cromlish W, Collins S, Loy AL, Normandin D, Cheng A, Himms-Hagen J, Chan CC, et al. Increased insulin sensitivity and obesity resistance in mice lacking the protein tyrosine phosphatase-1B gene. Science 1999;283:1544–1548. [PubMed: 10066179]

Galic S, Hauser C, Kahn BB, Haj FG, Neel BG, Tonks NK, Tiganis T. Coordinated Regulation of Insulin Signaling by the Protein Tyrosine Phosphatases PTP1B and TCPTP. Mol Cell Biol 2005;25:819–829. [PubMed: 15632081]

Haber CA, Lam TK, Yu Z, Gupta N, Goh T, Bogdanovic E, Giacca A, Fantus IG. N-acetylcysteine and taurine prevent hyperglycemia-induced insulin resistance in vivo: possible role of oxidative stress. Am J Physiol Endocrinol Metab 2003;285:E744–753. [PubMed: 12799318]

Ho YS, Magnenat JL, Bronson RT, Cao J, Gargano M, Sugawara M, Funk CD. Mice deficient in cellular glutathione peroxidase develop normally and show no increased sensitivity to hyperoxia. J Biol Chem 1997;272:16644–16651. [PubMed: 9195979]

Houstis N, Rosen ED, Lander ES. Reactive oxygen species have a causal role in multiple forms of insulin resistance. Nature 2006;440:944–948. [PubMed: 16612386]

Hughes WE, Cooke FT, Parker PJ. Sac phosphatase domain proteins. Biochem J 2000;350(Pt 2):337–352. [PubMed: 10947947]

Kim JA, Wei Y, Sowers JR. Role of mitochondrial dysfunction in insulin resistance. Circ Res 2008;102:401–414. [PubMed: 18309108]

NIH-PA Author Manuscript

NIH-PA Author Manuscript

NIH-PA Author Manuscript

Kim YI, Lee FN, Choi WS, Lee S, Youn JH. Insulin regulation of skeletal muscle PDK4 mRNA expression is impaired in acute insulin-resistant states. Diabetes 2006;55:2311–2317. [PubMed: 16873695]

Kong AM, Speed CJ, O'Malley CJ, Layton MJ, Meehan T, Loveland KL, Cheema S, Ooms LM, Mitchell CA. Cloning and characterization of a 72-kDa inositol-polyphosphate 5-phosphatase localized to the Golgi network. J Biol Chem 2000;275:24052–24064. [PubMed: 10806194]

Kwon J, Lee SR, Yang KS, Ahn Y, Kim YJ, Stadtman ER, Rhee SG. Reversible oxidation and inactivation of the tumor suppressor PTEN in cells stimulated with peptide growth factors. Proc Natl Acad Sci U S A 2004;101:16419–16424. [PubMed: 15534200]

Larance M, Ramm G, Stockli J, van Dam EM, Winata S, Wasinger V, Simpson F, Graham M, Junutula JR, Guilhaus M, et al. Characterization of the role of the Rab GTPase-activating protein AS160 in insulin-regulated GLUT4 trafficking. J Biol Chem 2005;280:37803–37813. [PubMed: 16154996]

Lazar DF, Saltiel AR. Lipid phosphatases as drug discovery targets for type 2 diabetes. Nat Rev Drug Discov 2006;5:333–342. [PubMed: 16582877]

Lee FN, Zhang L, Zheng D, Choi WS, Youn JH. Insulin suppresses PDK-4 expression in skeletal muscle independently of plasma FFA. Am J Physiol Endocrinol Metab 2004;287:E69–74. [PubMed: 15026305]

Lee SR, Yang KS, Kwon J, Lee C, Jeong W, Rhee SG. Reversible inactivation of the tumor suppressor PTEN by H2O2. J Biol Chem 2002;277:20336–20342. [PubMed: 11916965]

Mahadev K, Motoshima H, Wu X, Ruddy JM, Arnold RS, Cheng G, Lambeth JD, Goldstein BJ. The NAD(P)H oxidase homolog Nox4 modulates insulin-stimulated generation of H2O2 and plays an integral role in insulin signal transduction. Mol Cell Biol 2004;24:1844–1854. [PubMed: 14966267]

McClung JP, Roneker CA, Mu W, Lisk DJ, Langlais P, Liu F, Lei XG. Development of insulin resistance and obesity in mice overexpressing cellular glutathione peroxidase. Proc Natl Acad Sci U S A 2004;101:8852–8857. [PubMed: 15184668]

Meng TC, Buckley DA, Galic S, Tiganis T, Tonks NK. Regulation of Insulin Signaling through Reversible Oxidation of the Protein-tyrosine Phosphatases TC45 and PTP1B. J Biol Chem 2004;279:37716–37725. [PubMed: 15192089]

Newsholme P, Haber EP, Hirabara SM, Rebelato EL, Procopio J, Morgan D, Oliveira-Emilio HC, Carpinelli AR, Curi R. Diabetes associated cell stress and dysfunction: role of mitochondrial and non-mitochondrial ROS production and activity. J Physiol 2007;583:9–24. [PubMed: 17584843]

Ooms LM, Horan KA, Rahman P, Seaton G, Gurung R, Kethesparan DS, Mitchell CA. The role of the inositol polyphosphate 5-phosphatases in cellular function and human disease. Biochem J 2009;419:29–49. [PubMed: 19272022]

Rhee SG. Cell signaling. H2O2, a necessary evil for cell signaling. Science 2006;312:1882–1883. [PubMed: 16809515]

Ristow M, Zarse K, Oberbach A, Kloting N, Birringer M, Kiehntopf M, Stumvoll M, Kahn CR, Bluher M. Antioxidants prevent health-promoting effects of physical exercise in humans. Proc Natl Acad Sci U S A 2009;106:8665–8670. [PubMed: 19433800]

Rui L, Aguirre V, Kim JK, Shulman GI, Lee A, Corbould A, Dunaif A, White MF. Insulin/IGF-1 and TNF-alpha stimulate phosphorylation of IRS-1 at inhibitory Ser307 via distinct pathways. J Clin Invest 2001;107:181–189. [PubMed: 11160134]

Sandstrom ME, Zhang SJ, Bruton J, Silva JP, Reid MB, Westerblad H, Katz A. Role of reactive oxygen species in contraction-mediated glucose transport in mouse skeletal muscle. J Physiol 2006;575:251–262. [PubMed: 16777943]

Sano H, Kane S, Sano E, Miinea CP, Asara JM, Lane WS, Garner CW, Lienhard GE. Insulin-stimulated phosphorylation of a Rab GTPase-activating protein regulates GLUT4 translocation. J Biol Chem 2003;278:14599–14602. [PubMed: 12637568]

Schroder E, Eaton P. Hydrogen peroxide as an endogenous mediator and exogenous tool in cardiovascular research: issues and considerations. Curr Opin Pharmacol 2008;8:153–159. [PubMed: 18243791]

Seo JH, Ahn Y, Lee SR, Yeol Yeo C, Chung Hur K. The major target of the endogenously generated reactive oxygen species in response to insulin stimulation is phosphatase and tensin homolog and not phosphoinositide-3 kinase (PI-3 kinase) in the PI-3 kinase/Akt pathway. Mol Biol Cell 2005;16:348–357. [PubMed: 15537704]

NIH-PA Author Manuscript

NIH-PA Author Manuscript

NIH-PA Author Manuscript

Shields BJ, Hauser C, Bukczynska PE, Court NW, Tiganis T. DNA replication stalling attenuates tyrosine kinase signaling to suppress S phase progression. Cancer Cell 2008;14:166–179. [PubMed: 18691551]

Tiganis T, Bennett AM, Ravichandran KS, Tonks NK. Epidermal growth factor receptor and the adaptor protein p52^{Shc} are specific substrates of T-cell protein tyrosine phosphatase. Mol Cell Biol 1998;18:1622–1634. [PubMed: 9488479]

Tonks NK. Protein tyrosine phosphatases: from genes, to function, to disease. Nat Rev Mol Cell Biol 2006;7:833–846. [PubMed: 17057753]

Ushio-Fukai M. Localizing NADPH oxidase-derived ROS. Sci STKE 2006;2006:re8. [PubMed: 16926363]

Veal EA, Day AM, Morgan BA. Hydrogen peroxide sensing and signaling. Mol Cell 2007;26:1–14. [PubMed: 17434122]

Wang XD, Vatamaniuk MZ, Wang SK, Roneker CA, Simmons RA, Lei XG. Molecular mechanisms for hyperinsulinaemia induced by overproduction of selenium-dependent glutathione peroxidase-1 in mice. Diabetologia 2008;51:1515–1524. [PubMed: 18560803]

Watt MJ, Dzamko N, Thomas WG, Rose-John S, Ernst M, Carling D, Kemp BE, Febbraio MA, Steinberg GR. CNTF reverses obesity-induced insulin resistance by activating skeletal muscle AMPK. Nat Med 2006;12:541–548. [PubMed: 16604088]

Weyer C, Hanson RL, Tataranni PA, Bogardus C, Pratley RE. A high fasting plasma insulin concentration predicts type 2 diabetes independent of insulin resistance: evidence for a pathogenic role of relative hyperinsulinemia. Diabetes 2000;49:2094–2101. [PubMed: 11118012]

Wijesekara N, Konrad D, Eweida M, Jefferies C, Liadis N, Giacca A, Crackower M, Suzuki A, Mak TW, Kahn CR, et al. Muscle-specific Pten deletion protects against insulin resistance and diabetes. Mol Cell Biol 2005;25:1135–1145. [PubMed: 15657439]

Wojtaszewski JF, Higaki Y, Hirshman MF, Michael MD, Dufresne SD, Kahn CR, Goodyear LJ. Exercise modulates postreceptor insulin signaling and glucose transport in muscle-specific insulin receptor knockout mice. J Clin Invest 1999;104:1257–1264. [PubMed: 10545524]

Wojtaszewski JF, Jorgensen SB, Frosig C, MacDonald C, Birk JB, Richter EA. Insulin signalling: effects of prior exercise. Acta Physiol Scand 2003;178:321–328. [PubMed: 12864736]

Zhou Q, Dohm GL. Treadmill running increases phosphatidylinostol 3-kinase activity in rat skeletal muscle. Biochem Biophys Res Commun 1997;236:647–650. [PubMed: 9245706]

NIH-PA Author Manuscript

NIH-PA Author Manuscript

NIH-PA Author Manuscript

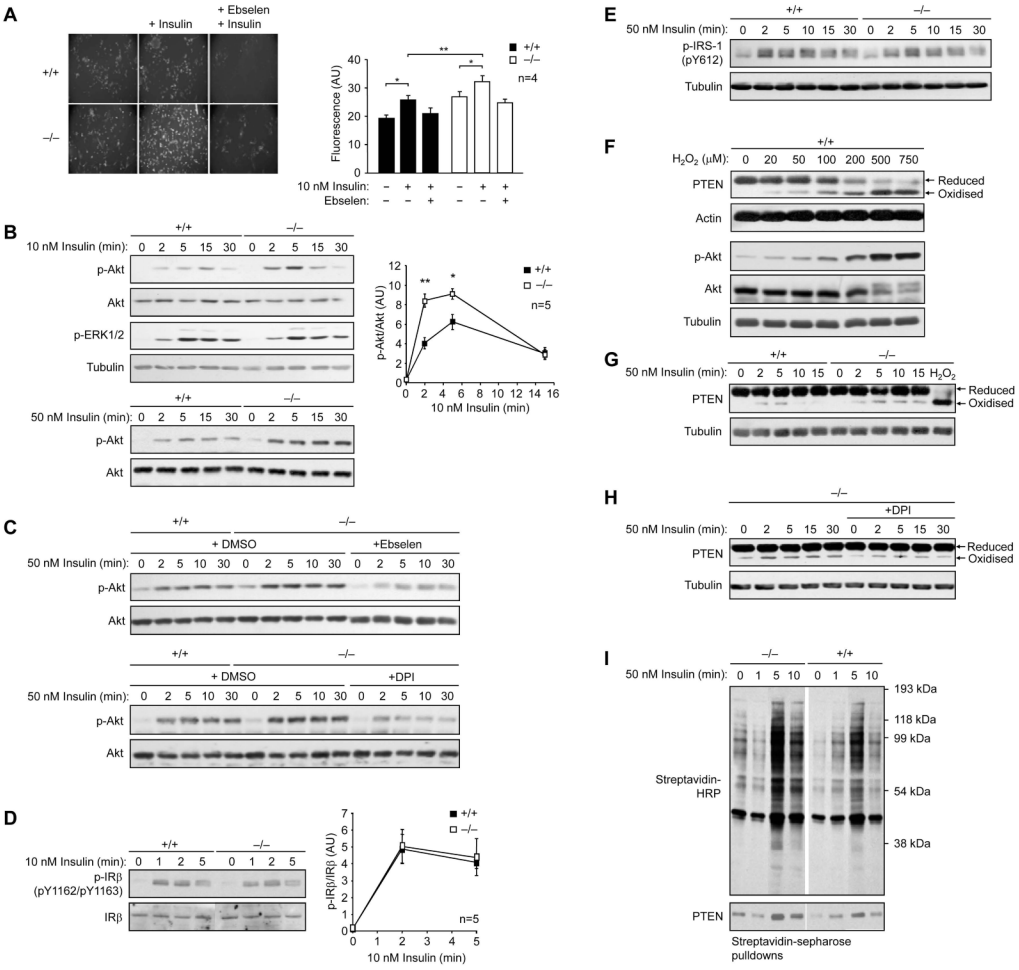

Figure 1. Enhanced insulin-induced ROS generation in Gpx1−/− cells results in PTEN oxidation and elevated PI3K/Akt signaling

(**a**) MEFs were serum starved for 4 h, pretreated with vehicle control or ebselen (10 μM, 40 min), left unstimulated or stimulated with insulin (10 min, 5 min), CM-H_2DCF-DA (10 μM, 10 min) added and DCF fluorescence assessed; arbitrary units (AU) are shown. (**b–e**) MEFs were serum starved, stimulated with insulin and processed for immunoblot analysis with antibodies to the Y1162/Y1163 phosphorylated IR β-subunit (p-IRβ), Y612 phosphorylated IRS-1 (p-IRS-1), Ser-473 phosphorylated Akt (p-Akt), or the phosphorylated MAPK ERK1/2 (p-ERK1/2) and then reprobed as indicated. Where indicated cells were pretreated with ebselen (10 μM, 40 min) or DPI (100 μM, 30 min). In **b** and **d** p-Akt or p-IRβ were quantified and normalised for Akt and IRβ respectively. **(f)** Gpx1 +/+ MEFs were serum starved and then stimulated with H_2O_2 for 5 min, lysed in the presence of 50 mM N-ethylmaleimide (NEM) to irreversibly alkylate free Cys and prevent the oxidation of Cys post lysis and processed for immunoblot analysis. Indicated are the reduced and oxidized (inactive) forms of PTEN. (**g–h**) Gpx1−/− and +/+ MEFs were serum starved, pre-incubated with vehicle control or DPI, stimulated, lysed in the presence of NEM and processed for immunoblot analysis. Results shown are representative of three independents experiments. (**i**) Gpx1−/− and +/+ MEFs were serum starved and then stimulated with insulin. Cells were lysed and oxidised PTPs labelled with the sulfhydryl reactive probe BPP-biotin and subjected to streptavidin-sepharose pull downs and processed for immunoblot analysis. Results shown in **a, b & d** are means ± SE

NIH-PA Author Manuscript

NIH-PA Author Manuscript

NIH-PA Author Manuscript

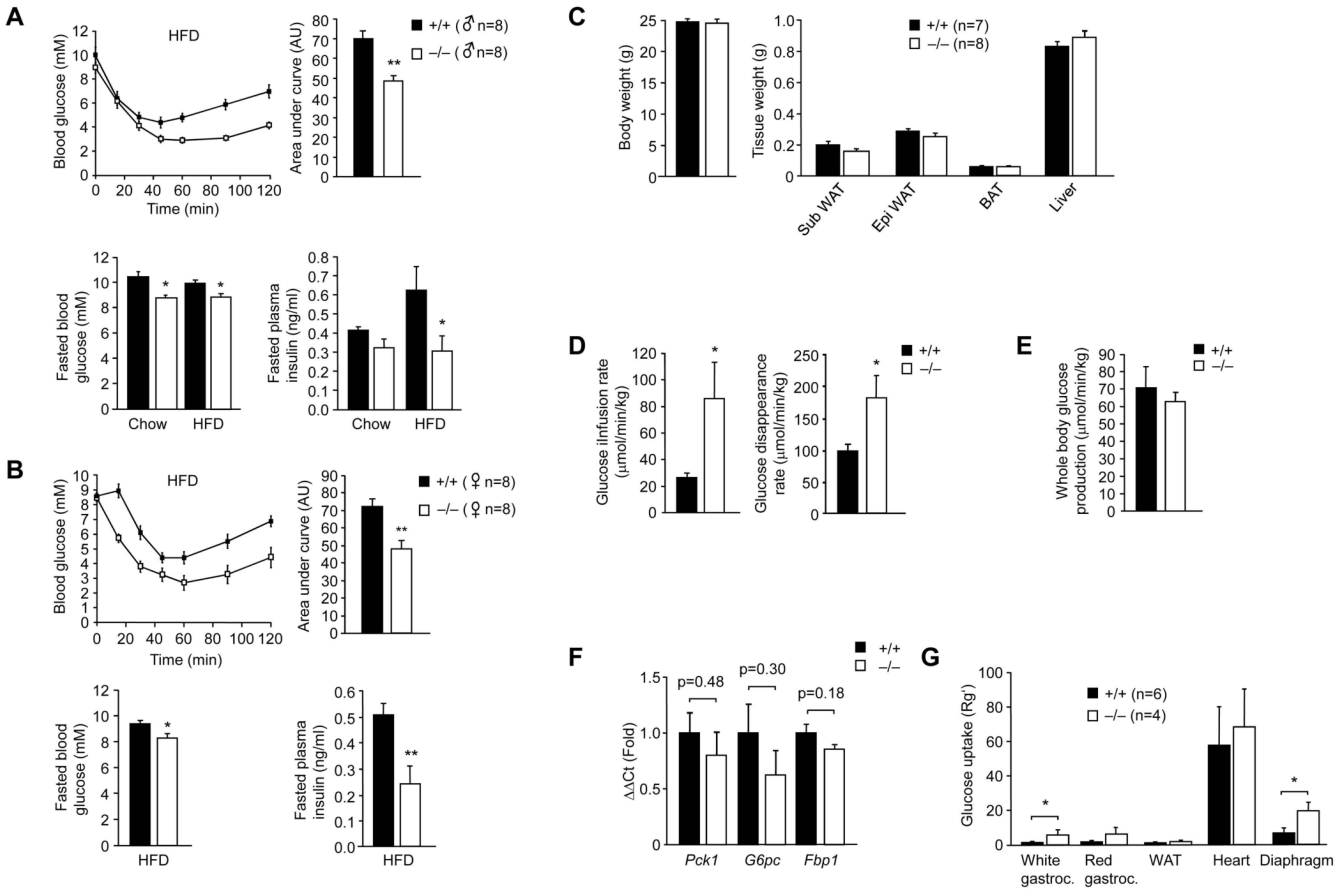

Figure 2. Insulin sensitivity is enhanced in Gpx1−/− mice

8–10 week old Gpx1−/− and +/+ (**a**) male and (**b**) female mice were fed a HFD or standard chow diet for 12 weeks. Mice were fasted either for 6 h and blood glucose and plasma insulin levels measured, or 4 h and ITTs performed (0.65 mU insulin/g body weight). Areas under ITT curves were determined. (**c–g**) 8–10 week old Gpx1−/− and +/+ male mice were fed a HFD for 12 weeks and hyperinsulinemic-euglycemic clamps performed on weight-matched mice. (**d**) Glucose infusion and disappearance rates were determined and (**e**) whole body glucose production determined by subtracting the glucose infusion rate from the glucose appearance rate. (**f**) Livers were harvested at the end of the clamp and processed for quantitative (ΔΔCt) real time PCR to measure the expression of the gluconeogenic genes *G6pc* (+/+ n=8, −/− n=7), *Pck1* (+/+ n=6, −/− n=5) and *Fbp1* (+/+ n=9, −/− n=8). (**g**) The uptake of glucose into white and red *gastrocnemius* (Gastroc) and diaphragm skeletal muscles, heart and white adipose tissue (epididymal; WAT) was assessed by administrating 2-deoxy-[1-^{14}C]glucose at the end of the clamp. Results shown in **a**–**g** are means ± SE.

NIH-PA Author Manuscript
NIH-PA Author Manuscript
NIH-PA Author Manuscript

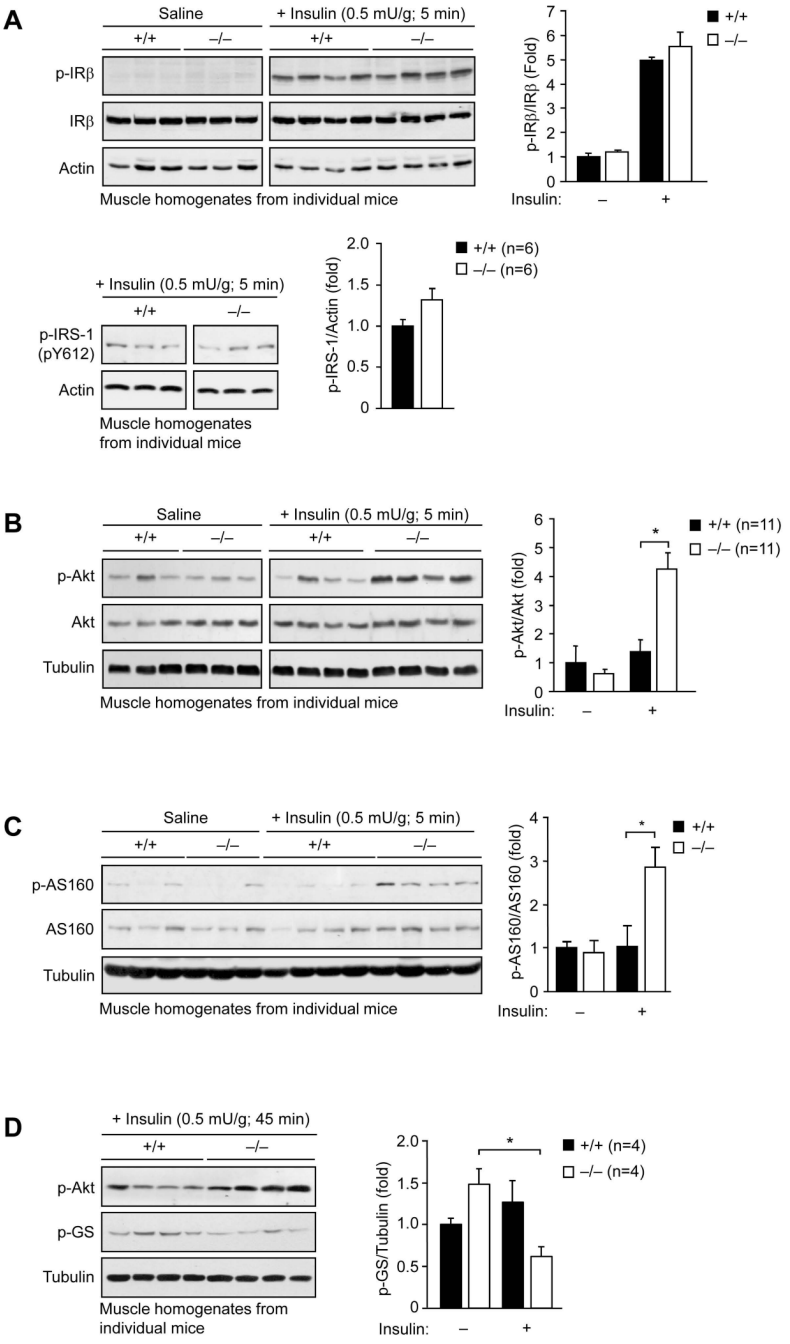

Figure 3. Enhanced insulin-induced PI3K/Akt signaling in Gpx1−/− muscle

8–10 week old Gpx1−/− and +/+ male mice were fed a HFD for 12 weeks, fasted for 4 h, injected with saline or insulin (0.5 mU/g, intraperitoneal) and *gastrocnemius* muscle extracted, homogenised and insulin signaling in individual mice assessed by immunoblot analysis and quantified by densitometry. Results shown are means ± SE.

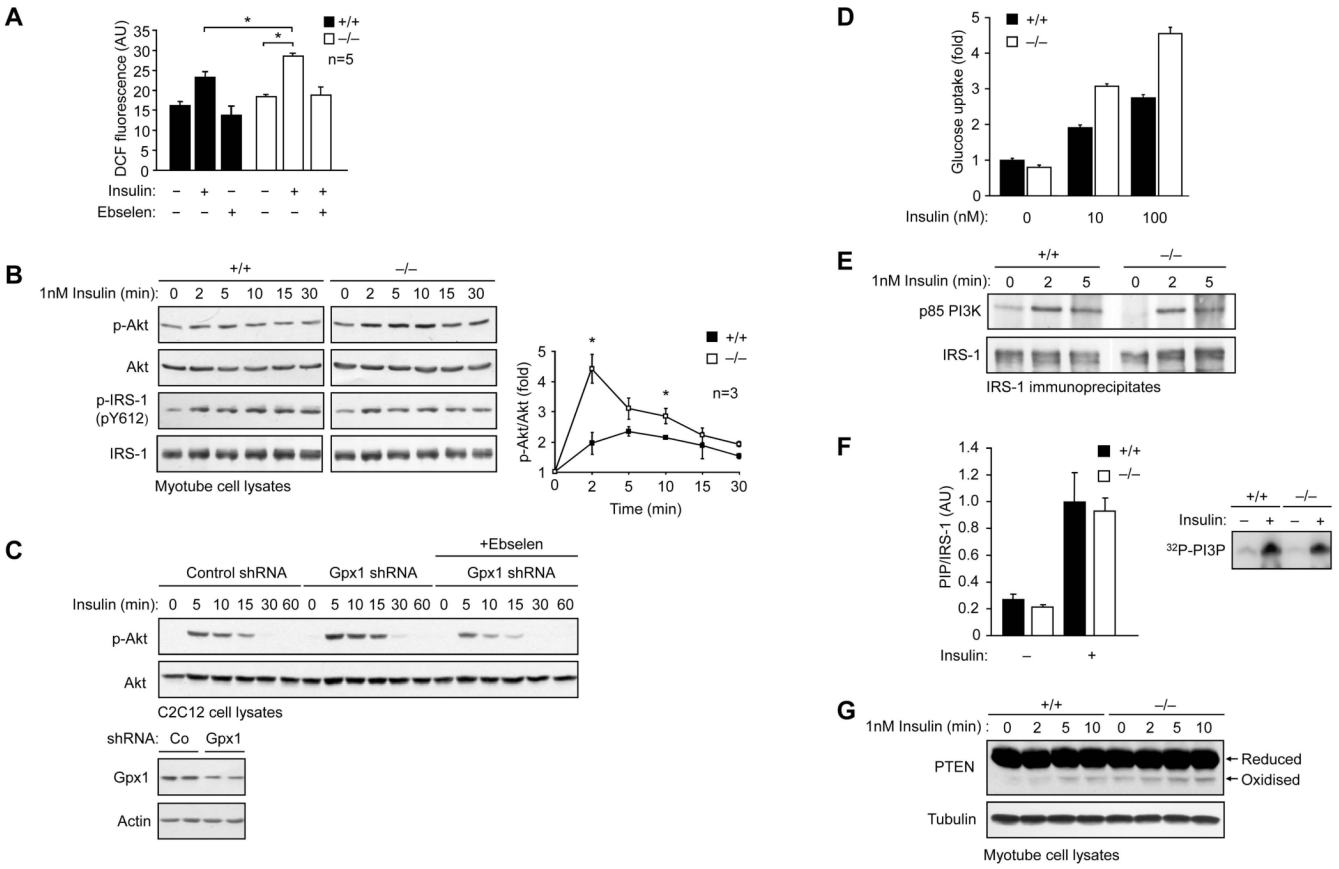

Figure 4. Enhanced insulin-induced ROS, PI3K/Akt signaling, PTEN oxidation and glucose uptake in Gpx1-deficient muscle cells

(**a**) Gpx1−/− and +/+ myoblasts were differentiated into myotubes, serum starved, pretreated with vehicle control or ebselen (10 μM, 40 min) and then either left unstimulated or stimulated with 1 nM insulin for 5 min before the addition of CM-H_2DCF-DA (10 μM, 10 min) and the quantification of DCF fluorescence. (**b**) Serum starved Gpx1 −/− and +/+ myotubes were stimulated with 1 nM insulin for the indicated times and processed for immunoblot analysis. Results shown are representative of three independent experiments. p-Akt was quantified by densitometric analysis and normalised for total Akt. (**c**) C2C12 cells transduced with control or Gpx1 shRNA lentiviral particles were serum starved for 6 h, pre-treated with vehicle control or ebselen and stimulated with 1 nM insulin for 10 min. Medium was then replenished and cells collected at the indicated times for immunoblot analysis. (**d**) Gpx1−/− and +/+ myotubes were serum starved in medium with no glucose for 4 h, stimulated with insulin for 30 min, medium removed and incubated with 2-Deoxy-D-[2,6-3H]glucose (1 μCi/mL) and incorporated radioactivity measured after 10 min. Results are means ± SD from sixtuplicate stimulations and are representative of two independent experiments. (**e**) Serum starved Gpx1 −/− and +/+ myotubes were stimulated with 1 nM insulin for the indicated times, IRS-1 immunoprecipitated and the association of the p85 subunit of PI3K monitored by immunoblot analysis. Results shown are representative of three independents experiments. (**f**) Serum starved myotubes were stimulated with 50 nM insulin for 10 min, IRS-1 immunoprecipitated and associated PI3K activity monitored and quantified as described in the methods; results are means ± SD from triplicate immunoprecipitations and are representative of two independent experiments. *Insert:* representative ^{32}P-phosphatidylinositol 3-phosphate (PI3P) generation by the immunoprecipitated PI3K. (**g**) Serum starved Gpx1−/− and +/+ myotubes were stimulated

NIH-PA Author Manuscript NIH-PA Author Manuscript NIH-PA Author Manuscript

with 1 nM insulin for the indicated times, lysed in the presence of NEM and processed for immunoblot analysis with antibodies to PTEN. Indicated are the reduced and oxidized (inactive) forms of PTEN. Results shown are representative of three independents experiments.

NIH-PA Author Manuscript
NIH-PA Author Manuscript
NIH-PA Author Manuscript

NIH-PA Author Manuscript

NIH-PA Author Manuscript

NIH-PA Author Manuscript

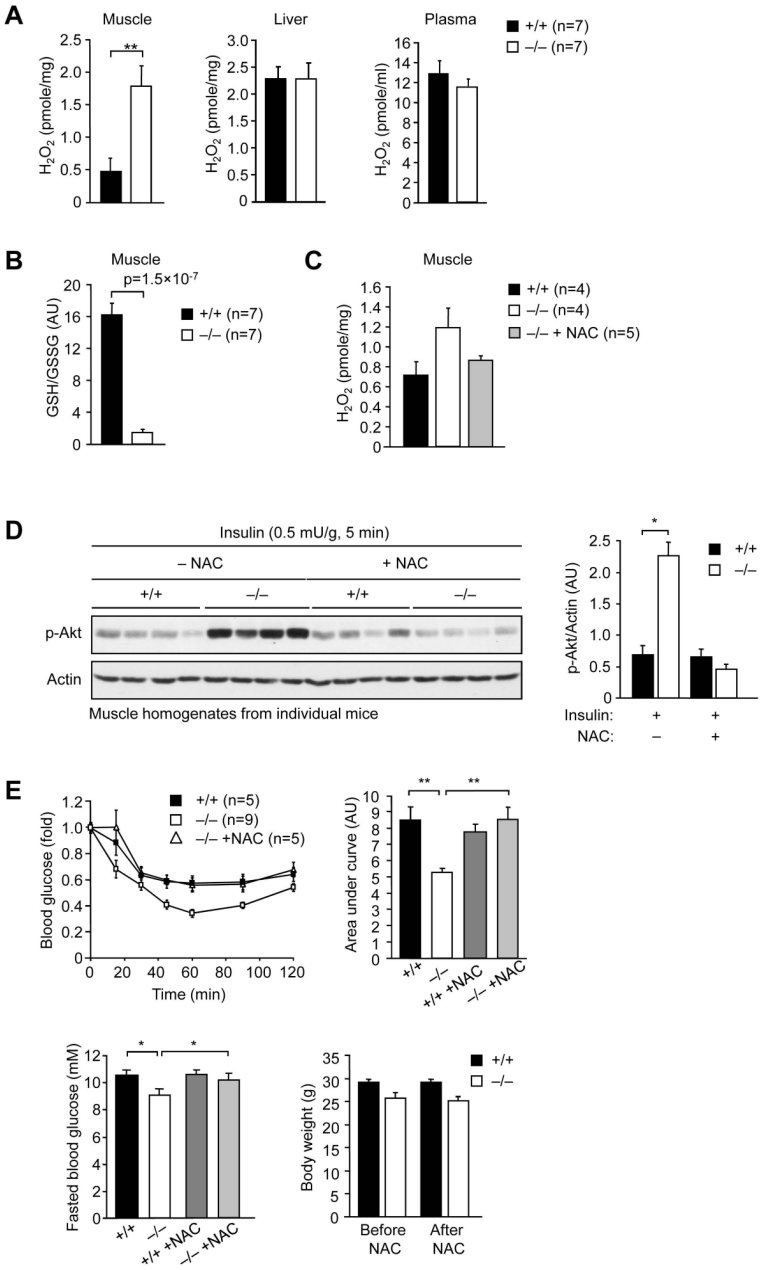

Figure 5. The enhanced PI3K/Akt signaling and insulin sensitivity in Gpx1−/− mice can be attenuated by the anti-oxidant N-acetylcysteine

8–10 week old Gpx1−/− and +/+ male mice were fed a HFD for 12 weeks and either left untreated or administered NAC for seven days (10 mg/L in drinking water). (**a, c**) H_2O_2 levels in liver, gastrocnemius muscle or blood plasma from fasted and insulin stimulated mice were determined using Amplex Red and normalised to the sample protein content or volume. (**b**) GSH/GSSG ratios were determined in muscle extracts. (**d**) Mice were fasted, injected with saline or insulin and gastrocnemius muscle extracted, homogenised and p-Akt signaling in individual mice assessed by immunoblot analysis and quantified by densitometry. (**e**) Insulin sensitivity in untreated −/− versus +/+ mice, or mice administered NAC was determined by performing ITTs (0.65 mU/g). Areas under ITT curves were determined; for clarity ITT curves for NAC treated +/+ mice are not shown. The corresponding fasted blood glucose levels and

NIH-PA Author Manuscript

NIH-PA Author Manuscript

NIH-PA Author Manuscript

body weights determined before and after NAC treatment are also shown. Results in **a–e** are means ± SE.

NIH-PA Author Manuscript

NIH-PA Author Manuscript

NIH-PA Author Manuscript

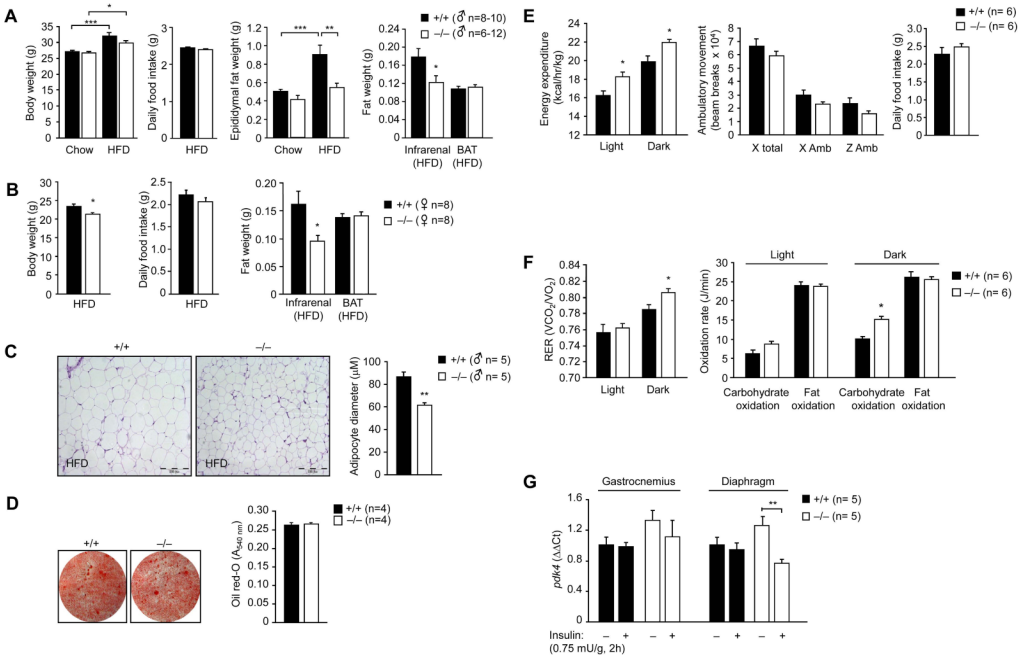

Figure 6. Obesity resistance and increased energy expenditure in Gpx1−/− mice

8–10 week old (**a & c**) male and (**b**) female mice were fed a HFD, or where indicated a standard chow diet, for 12 weeks. Mice were weighed and epididymal, infrarenal and brown adipose (BAT) tissues extracted and weighed. In **c** epididymal fat tissues were processed for immunohistochemistry (hematoxylin and eosin staining). The cross-sectional diameters of adipocytes (100 cells per mouse) were determined using Image J software (NIH). Represenative micrographs and the quantified results are shown. (**d**) Gpx1−/− and +/+ MEFs were differentiated into adipocytes and stained with oil red-O to monitor lipid content. Representative micrographs and quantified results are shown. (**e**) 8–10 week old Gpx1−/− (n = 6) and +/+ (n = 6) male littermates were fed a HFD for 12 weeks and energy expenditure during the light and dark cycles, ambulatory movement (x and y axes) and daily food intake monitored over 48 h. (**f**) 8–10 week old Gpx1−/− (n = 6) and +/+ (n = 6) male littermates were fed a HFD for 12 weeks and gas exchange data used to calculate the respiratory exchange ratio (RER = VO_2/VCO_2). Carbohydrate versus fat oxidation rates were calculated and expressed as Joules/min. (**g**) 8–10 week old Gpx1−/− and +/+ male littermates were fed a HFD for 12 weeks, starved for 4 h, injected with saline or insulin (2h, 0.75 mU/g, intraperitoneal) and diaphragm or *gastrocnemius* muscle extracted and processed for real time PCR (ΔΔCt) to measure *pdk4* expression. Results are **a-g** means ± SE.

NIH-PA Author Manuscript

NIH-PA Author Manuscript

NIH-PA Author Manuscript

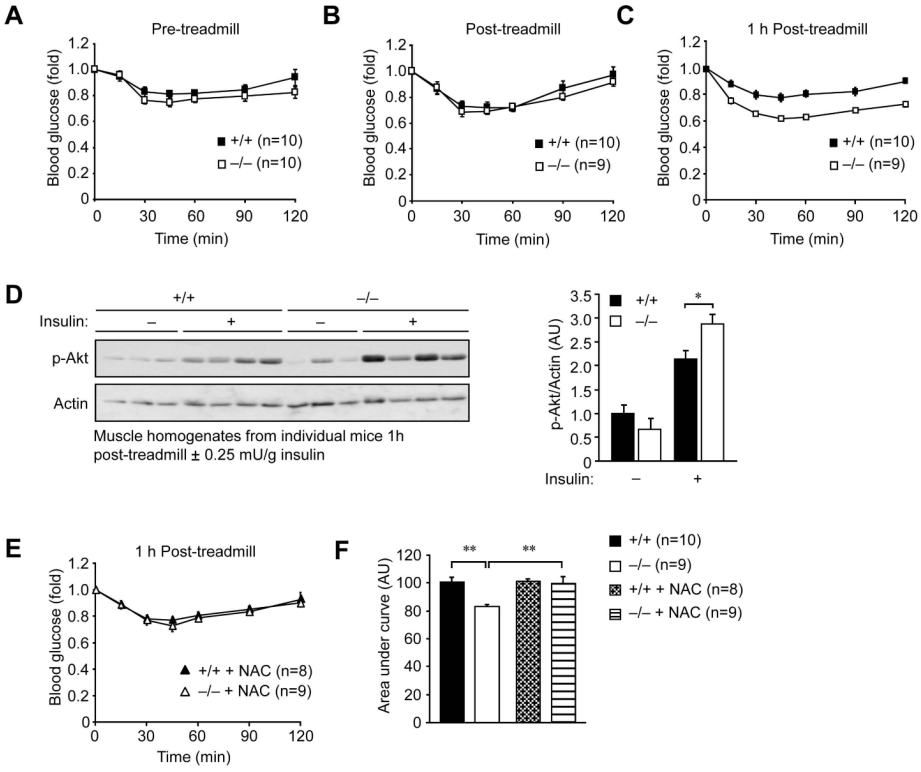

Figure 7. Sustained exercise-induced and ROS-mediated insulin sensitivity in Gpx1−/− mice

Chow fed 10–12 week old mice were starved overnight (12 h) and (**a**) ITTs (0.25 mU/g) performed, or otherwise (**b–c**) treadmill exercised (30 min running at 16 m/min at a 5° incline) and ITTs performed (**b**) immediately after or (**c**) after 1 h of rest. (**d**) *Gastrocnemius* muscle from exercised and 1 h rested mice injected with saline or insulin for 30 min was rapidly excised and processed for immunoblot analysis; results were quantified by densitometric analysis. (**e**) Mice from **c** were subsequently administered NAC for seven days (10 mg/L in drinking water), exercised, rested for 1 h and ITTs repeated. (**f**) Areas under ITT curves from **c** and **e** were determined. Results in **a**–**f** are means ± SE.